Cell Reports, Volume *32*

Supplemental Information

A Brainstem Locomotor Circuit Drives the Activity of Speed Cells in the Medial Entorhinal Cortex

Miguel M. Carvalho, Nouk Tanke, Emilio Kropff, Menno P. Witter, May-Britt Moser, and Edvard I. Moser

Figure S1

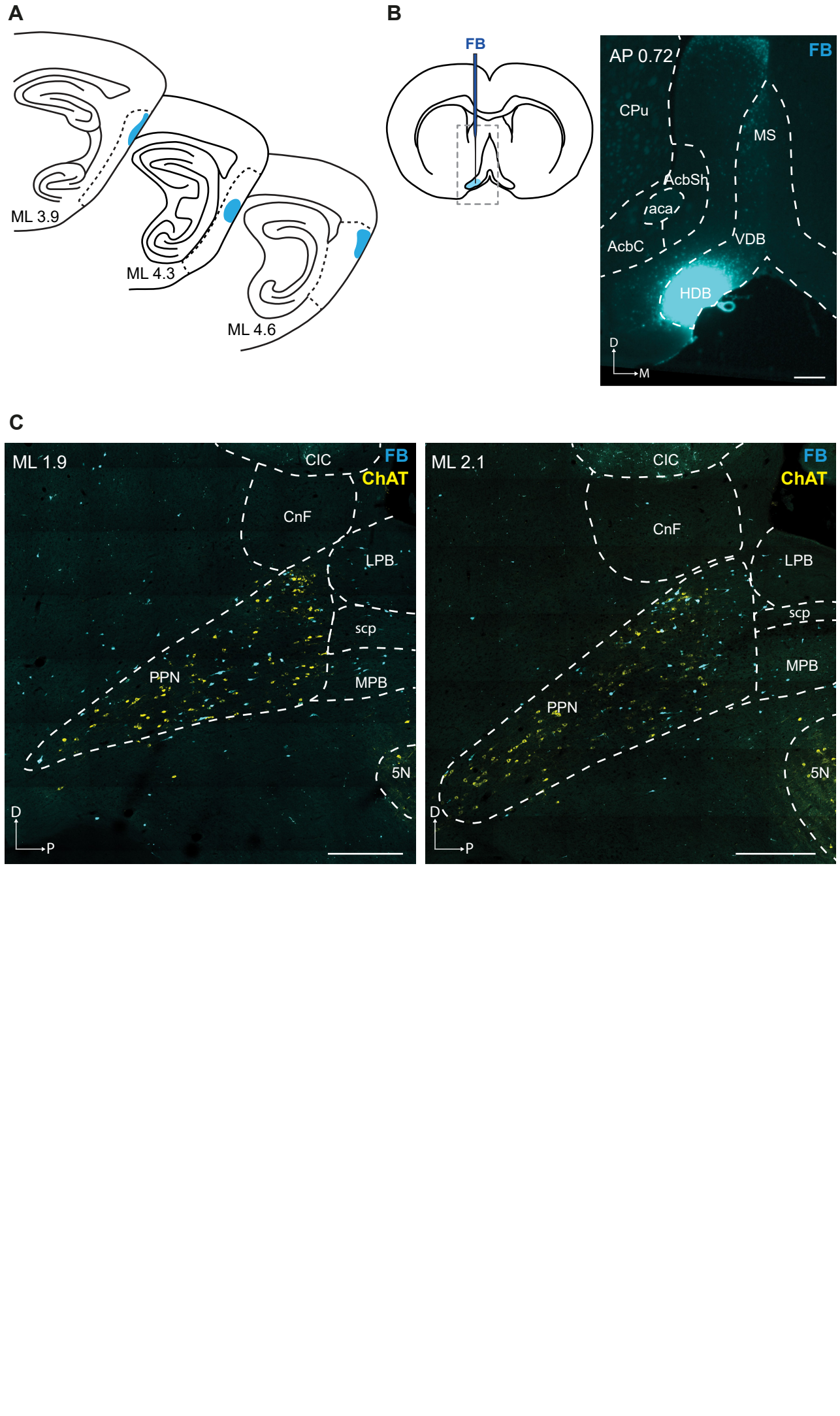
A
ML 3.9
ML 4.3
ML 4.6
B
FB
AP 0.72
FB
CPu
MS
AcbSh
aca
AcbC
VDB
HDB
D
M
C
ML 1.9
CIC
FB
ChAT
CnF
LPB
scp
PPN
MPB
5N
D
P
ML 2.1
CIC
FB
ChAT
CnF
LPB
scp
MPB
PPN
5N
D
P

Figure S1, related to Figure 1 | Fast blue injections in MEC and HDB. A. Schematic representation of sagittal sections for the three FB injections (blue circles) in MEC (black dashed line) performed in addition to the injection detailed in Figure 1A. Note that all four injections were located in the dorsal half of MEC, with a skew towards the dorsal end. **B.** Schematic coronal representation (left) and visualization of site for FB injection in HDB (right, cyan) (n = 1). **C.** Visualization of brainstem sagittal sections with FB-labelled neurons (blue) projecting to HDB (same experiment as **B**). Left and right panels show different mediolateral (ML) levels. Within the nuclei of the MLR (CnF and PPN), there was a substantial portion of FB-labeled neurons, identified based on ChAT immunofluorescence staining (yellow), despite the presence of some artefactual labeling (very bright fluorescent debris with equal luminance, but not having a soma shape or size and lacking an indication of a nucleus, particularly in the left panel). aca – anterior commissure, anterior part; AcbC – nucleus accumbens, core; AcbSh – nucleus accumbens, shell; CIC – central nucleus of the inferior colliculus; CnF – cuneiform nucleus; CPu – caudate putamen; HDB – diagonal band of Broca, horizontal limb; LPB – lateral parabrachial nucleus; MPB - medial parabrachial nucleus; MS – medial septum; PPN – pedunculopontine tegmental nucleus; scp – superior cerebellar peduncle; VDB – diagonal band of Broca, ventral limb; 5N – motor trigeminal nucleus. Note that PPN contains a core of scp fibers that are not separately delineated in the figure. Scale bars: 500 µm.

Figure S2

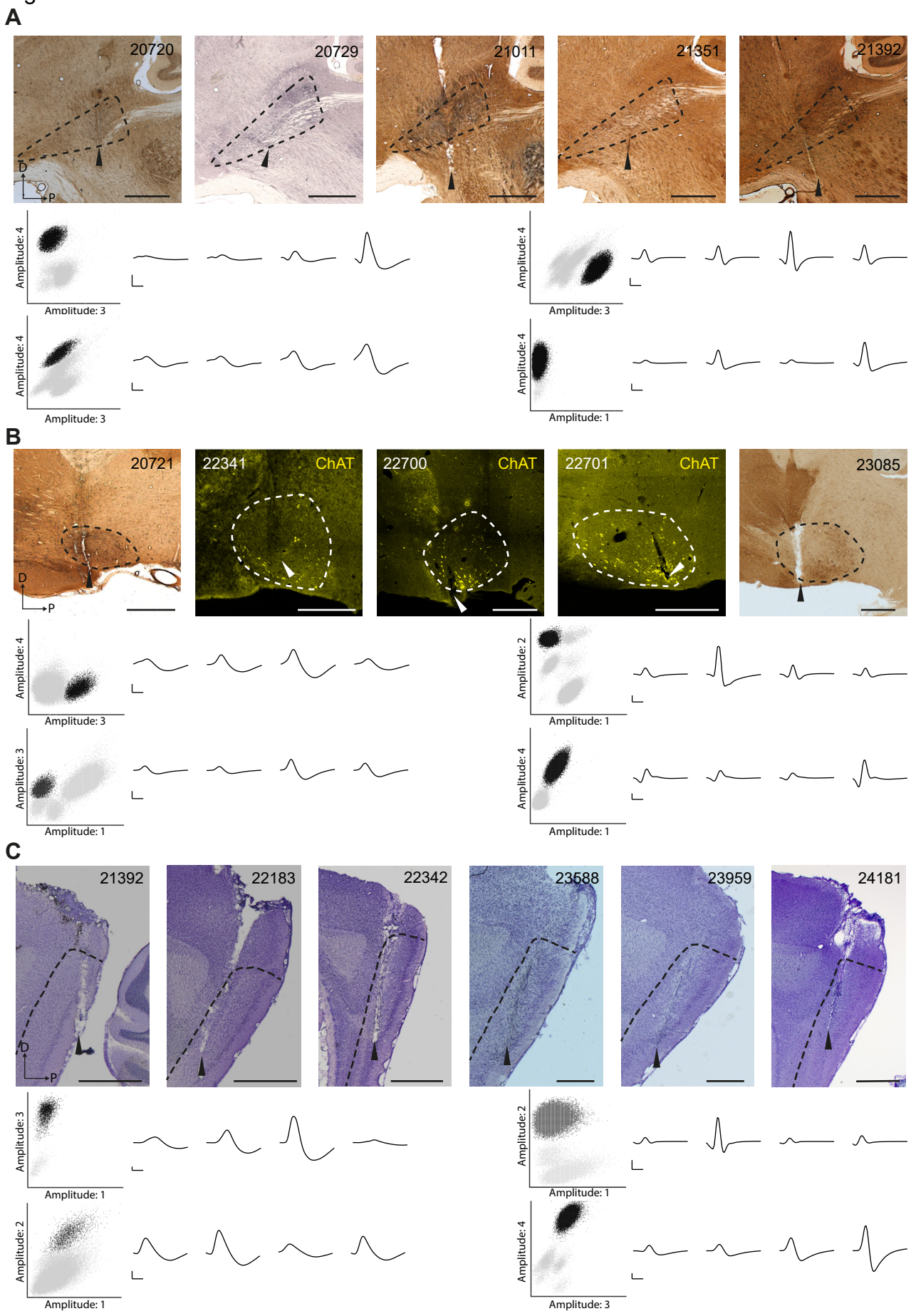
A
20720
20729
21011
21351
21392
D
P
Amplitude: 4
Amplitude: 3
Amplitude: 4
Amplitude: 3
Amplitude: 4
Amplitude: 1
B
20721
22341
ChAT
22700
ChAT
22701
ChAT
23085
D
P
Amplitude: 4
Amplitude: 3
Amplitude: 2
Amplitude: 1
Amplitude: 3
Amplitude: 1
Amplitude: 4
Amplitude: 1
C
21392
22183
22342
23588
23959
24181
D
P
Amplitude: 3
Amplitude: 1
Amplitude: 2
Amplitude: 1
Amplitude: 2
Amplitude: 1
Amplitude: 4
Amplitude: 3

Figure S2, related to Figure 2 and Figure 5 | Examples of recording tracks and spike cluster isolation and waveforms for speed cells in PPN, HDB and MEC. A. Top. Sagittal histology sections displaying additional representative examples of tetrode tracks for recordings performed in PPN. Animal number is shown in the top right of each image. Scale bars: 1 mm. Bottom. Representative examples of 2D spike projection diagrams and waveforms (mean ± SEM on each of the four electrodes of the tetrode) for two speed-modulated putative principal cells (left) and two speed-modulated putative interneurons (right), recorded in PPN. Spike projection diagrams show spike amplitudes on two selected channels. Black clusters correspond to waveforms shown to the right. Waveform scale bars represent 50 μV and 200 μs. **B.** Same as (**A**) for recordings in HDB. Scale bars: 500 μm. **C.** Same as (**A**) for recordings in MEC. Scale bars: 1 mm. For all histology panels, dashed lines indicate boundaries of the target region. PPN and HDB boundaries were defined based on AChE histochemical staining or ChAT immunofluorescence staining (the latter only for cases #22341, #22700 and #22701 in **B**), and MEC boundaries were defined based on Nissl staining. Black and white arrows identify final tetrode positions.

Figure S3

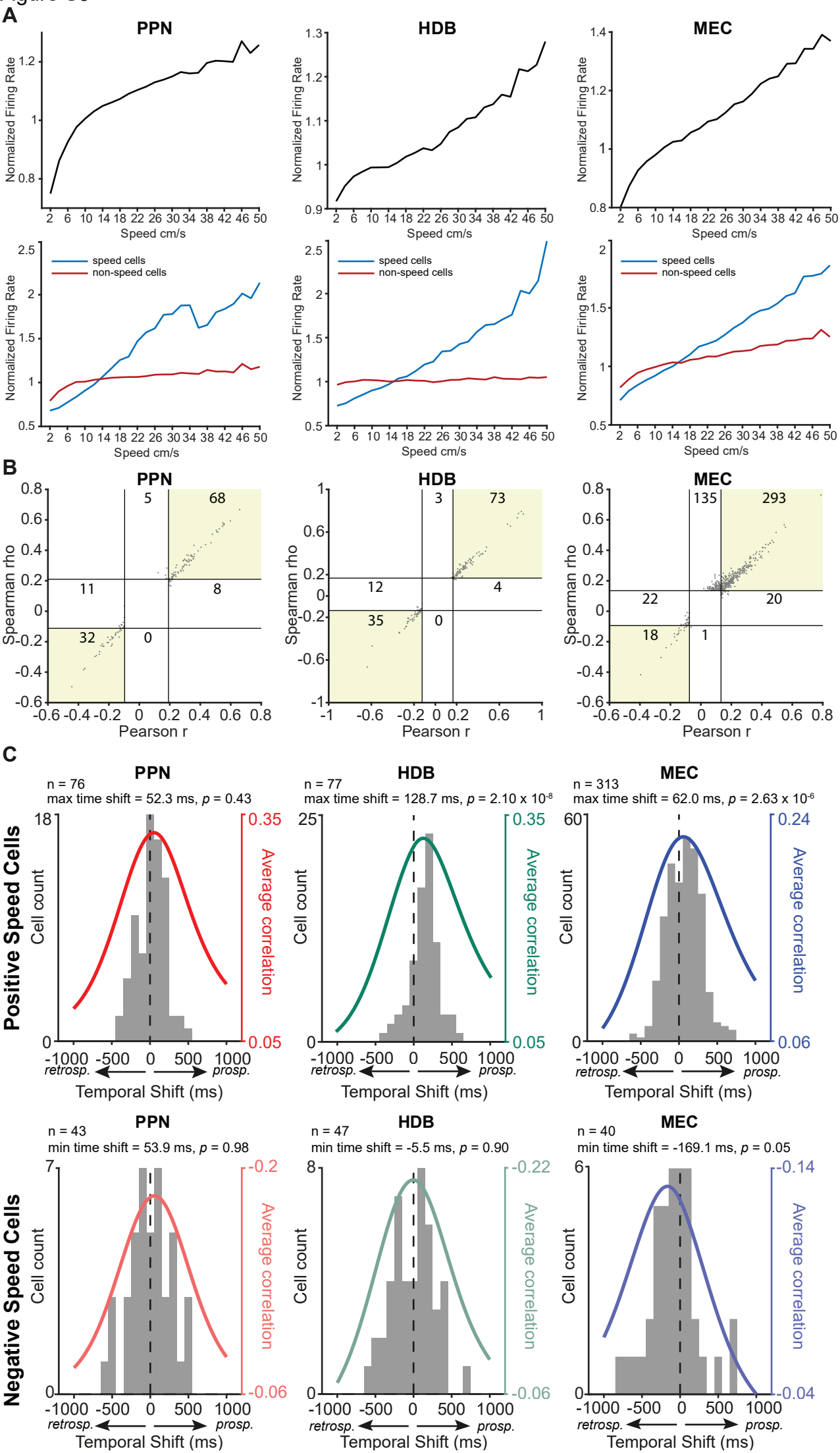
A
PPN
HDB
MEC
Normalized Firing Rate
Speed cm/s
speed cells
non-speed cells
B
PPN
HDB
MEC
Spearman rho
Pearson r
5
68
11
8
32
0
3
73
12
4
35
0
135
293
22
20
18
1
C
Positive Speed Cells
PPN
n = 76
max time shift = 52.3 ms, p = 0.43
HDB
n = 77
max time shift = 128.7 ms, p = 2.10 x 10-8
MEC
n = 313
max time shift = 62.0 ms, p = 2.63 x 10-6
Cell count
Average correlation
retrosp.
prosp.
Temporal Shift (ms)
Negative Speed Cells
PPN
n = 43
min time shift = 53.9 ms, p = 0.98
HDB
n = 47
min time shift = -5.5 ms, p = 0.90
MEC
n = 40
min time shift = -169.1 ms, p = 0.05

Figure S3, related to Figure 2 | Linearity and non-linearity of speed tuning and temporal bias of speed cell coding in PPN, HDB and MEC. A. Top. Representation of the change in normalized average firing rate (black line) as a function of running speed for the entire population of recorded cells in PPN (left), HDB (middle) and MEC (right). Note the change in population firing regimes in MEC at approximately 6 cm/s. A similar transition in firing regimes is also present in PPN and HDB around similar values of running speed. This threshold was used to define the lower boundary of the speed filter used for speed cell classification in all brain regions. Bottom. Representation of change in normalized average firing rate as a function of running speed for the entire population of classified speed cells (blue line, positive and negative cells pooled together) and non-speed cells (red line). **B.** Relationship between linear (Pearson's r) and non-linear (Spearman's rho) speed scores, for all speed cells (gray dots) identified with either correlation measure, in PPN (left), HDB (middle) and MEC (right). A 6 cm/s threshold was used in both cases. Vertical and horizontal lines represent the 1^{st} (vertical lines: left, horizontal lines: top) and 99^{th} (vertical lines: right, horizontal lines: bottom) percentile of the shuffled distribution of linear and non-linear speed scores, respectively, used to classify negative and positive speed cells with each of the methods. Cells were classified as exclusively linear (only passing Pearson threshold), exclusively nonlinear (only passing Spearman threshold) or mixed (passing both Pearson and Spearman thresholds). Number of cells falling into categories defined by the speed cell classification thresholds are shown. Yellow shaded areas identify quadrants with cells classified as negative speed cells (bottom left) or positive speed cells (top right) by both methods. Note, for all three brain regions, the overall similarity between linear and non-linear speed scores and the largely overlapping population of cells that each method classifies as speed cells (PPN - 81%, HDB - 85%, MEC - 64%). Note also that our method does not exclude that some signals with significant linear relationships might also (or better) be explained by a non-linear model. The number of cells with a significant speed relationship only with the linear model was for PPN: 19, HDB: 16, MEC: 42; the number of cells significant only with the nonlinear model was PPN: 5, HDB: 3, MEC: 136. In additional analyses, we used these classifications to compare the number of optogenetically responsive speed-modulated cells in HDB and MEC. In HDB, exclusively linear speed cells appeared to be more responsive to PPN stimulation than mixed speed cells (exclusively linear: 10/10; mixed: 37/58; Z = 2.3, P = 0.02, two proportions Z test), but not more responsive than the small number of exclusively nonlinear cells (exclusively linear: 10/10, exclusively nonlinear: 3/3). In MEC, exclusively linear speed cells were not more responsive than either mixed speed cells (exclusively linear: 4/17; mixed: 34/102; Z = 0.8, P = 0.4, two proportions Z test) or exclusively nonlinear (exclusively linear: 4/17, exclusively nonlinear: 4/33; Z = 1.0, P = 0.3, two proportions Z test). These comparisons show that for MEC, where we perform a more complete characterization of stimulation responses, the number of responsive speed cells is not dependent on whether the relationship to speed is purely linear or has additional nonlinear components. **C.** Panels show the temporal shift of spike data that maximized correlation between speed and firing rate for positive (top row) and negative (bottom row) speed cells in PPH (left), HDB (middle), and MEC (right). Temporal shifts were applied to the firing rate of each unit in 20 ms bins from -1000 ms to 1000 ms and correlations between speed and firing rate were determined for each speed cell and each shift. Histograms in gray show, for each temporal shift, the number of speed cells with maximal speed-rate correlation at that particular shift. Note that for each speed cell a different temporal shift maximizes speed-firing rate correlation. Superimposed curves represent for each temporal shift the average speed-firing rate correlation value for the whole population of speed cells. Numbers at the top of each panel indicate the interpolated temporal shift that maximizes, or minimizes, speed vs. rate correlations of the whole population (max/min time shift), together with significance of the comparison between the observed distribution of cell counts and a distribution with a median of 0 (Wilcoxon signed rank test). Although an overall prospective bias is present in positive speed cells in HDB ($n = 77$; $Z = 5.6$, $P = 2.10 \times 10^{-8}$) and MEC ($n = 313$; $Z = 4.7$, $P = 2.63 \times 10^{-6}$), a mixture of prospective and retrospective coding is seen in both classes of speed cells in all three regions. The precise assessment of distinct pathways for prospective speed coding along the PPN-HDB-MEC pathway is limited by the inability of our method to single out speed cells that are functionally connected between the three brain regions.

Figure S4

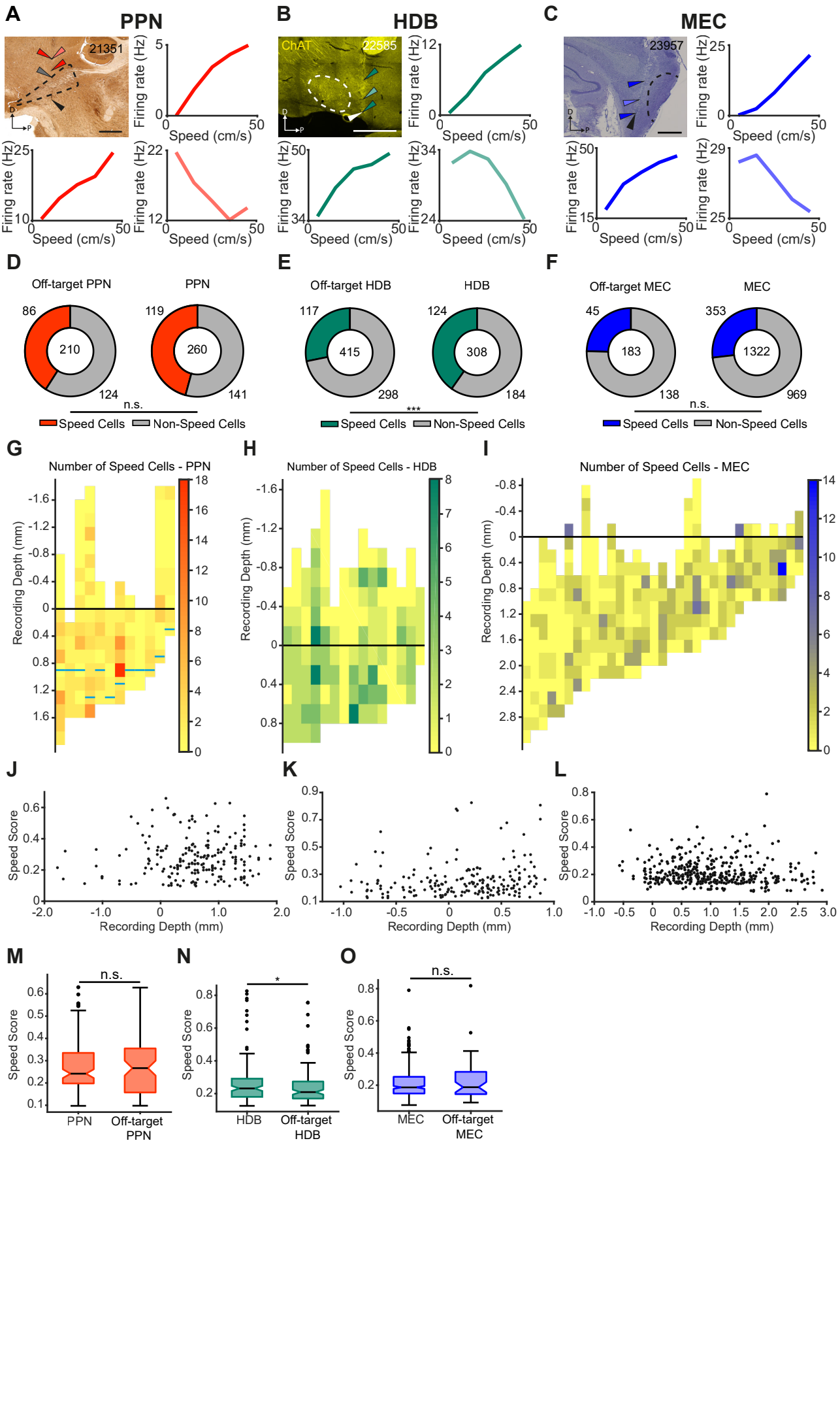
A
PPN
21351
B
HDB
ChAT
22585
C
MEC
23957
Firing rate (Hz)
Speed (cm/s)
D
Off-target PPN
PPN
86
210
124
119
260
141
n.s.
E
Off-target HDB
HDB
117
415
298
124
308
184
***
F
Off-target MEC
MEC
45
183
138
353
1322
969
n.s.
Speed Cells
Non-Speed Cells
G
Number of Speed Cells - PPN
H
Number of Speed Cells - HDB
I
Number of Speed Cells - MEC
Recording Depth (mm)
J
K
L
Speed Score
Recording Depth (mm)
M
N
O
n.s.
*
PPN
Off-target PPN
HDB
Off-target HDB
MEC
Off-target MEC

Figure S4, related to Figure 2 | Expression of locomotion speed in PPN, HDB and MEC off-target locations and anatomical distribution and speed modulation of speed cells along the dorsal-ventral axis of brainstem, basal forebrain and entorhinal cortex. A-C. Examples of sagittal histology sections (top left panel) displaying tetrode tracks for recordings in close proximity to PPN (**A**), HDB (**B**) and MEC (**C**), with examples of off-target positive and negative speed cells (top right and bottom panels). Rat number is indicated in the top right. Black or white arrows: final (deepest) tetrode location. Gray arrow: dorsal boundary of PPN in rat #21351. Colored arrows: approximate anatomical location where example speed cells were recorded. Scale bars: 1 mm. **D-F.** Proportion of speed and non-speed cells recorded in on and off-target regions of the brainstem (**D**), basal forebrain (**E**) and entorhinal cortex (**F**). Numbers in the center: total number of units recorded in each different region. A significantly higher proportion of speed cells was found within the target area compared to off-target areas for HDB, but not for PPN and MEC (PPN: off-target speed cells n = 86/210, PPN speed cells n = 119/260, Z = 1.1, P = 0.29; HDB: off-target speed cells n = 117/415, HDB speed cells n = 124/308, Z = 3.4, P = 6.8×10^{-4}; MEC: off-target speed cells n = 45/183, MEC speed cells n = 353/1322, Z = 0.6, P = 0.54, two proportions Z-test). *** P < 0.001, Z-score. **G-I.** Recording site reconstructions for each animal used in PPN (**G**), HDB (**H**) and MEC (**I**) recordings. Each column represents the recording track for one animal. The depth of each recording bin is expressed relative to the dorsal boundary of the respective target brain area (0, horizontal black line). Color code: number of speed cells in the bin. Short blue horizontal lines in **G**: approximate position of PPN ventral boundary. **J-L.** Relation between absolute speed modulation and recording depth for all speed cells recorded in the brainstem (**J**), basal forebrain (**K**) and entorhinal cortex (**L**) for all successfully targeted implants. Dorsal boundary of respective areas = 0, similar to **G-I**. **M-O.** Box plots showing absolute speed modulation of speed cells recorded off-target and inside the boundaries of PPN (**M**), HDB (**N**) and MEC (**O**). Line between box edges represent median; box edges represent 25th and 75th percentiles; whiskers, points within 1.5 times the interquartile range; black circles, outliers (applies to all box plots). In PPN and MEC, there was no differences in speed tuning of speed cells that were inside vs. outside the boundaries of these regions (PPN: off-target PPN n = 86, PPN n = 119, Z = 0.5, P = 0.61; MEC: off-target MEC n = 45, MEC n = 353, Z = 0.6, P = 0.54, Wilcoxon rank-sum test). In contrast, speed cells within the boundaries of HDB were more strongly modulated by running speed than surrounding speed cells (off-target HDB n = 117, HDB n = 124, Z = 2.1, P = 0.038, Wilcoxon rank-sum test). Collectively, the results in this figure show the presence of speed cells outside our target areas, and not only suggest that speed coding is widespread in the brain, but also hint that there might be parallel and complementary neuronal circuits for transmission of locomotor information beyond the areas targeted in the present study. * P < 0.05, Wilcoxon rank-sum test. For all analyses, positive and negative speed cells were pooled together.

Figure S5

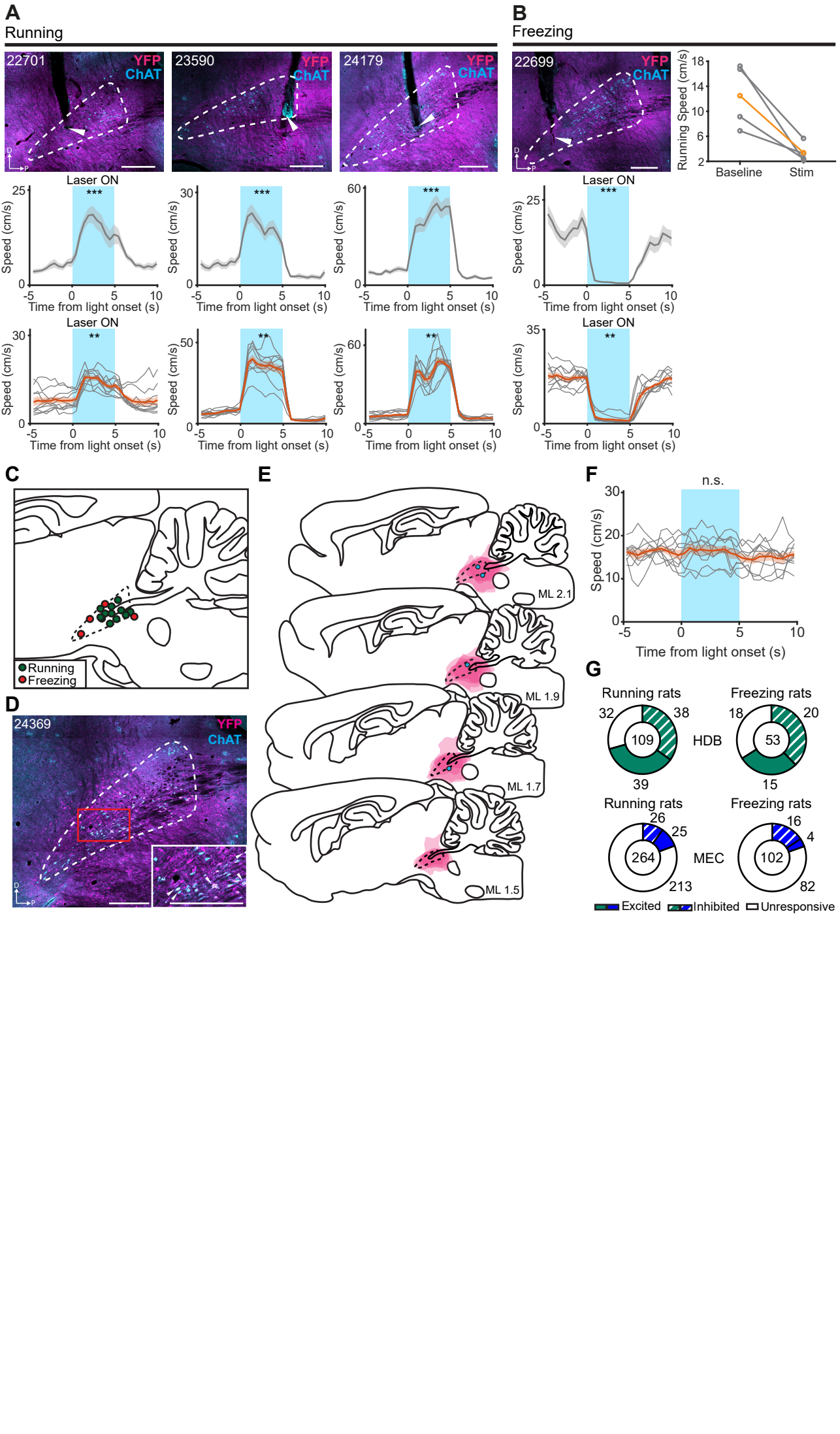
A
Running
B
Freezing
22701
23590
24179
22699
YFP
ChAT
Running Speed (cm/s)
Baseline
Stim
Laser ON
Speed (cm/s)
Time from light onset (s)
C
Running
Freezing
D
24369
E
ML 2.1
ML 1.9
ML 1.7
ML 1.5
F
n.s.
G
Running rats
Freezing rats
HDB
MEC
Excited
Inhibited
Unresponsive

Figure S5, related to Figure 3 and Figure 4 | ChR2 expression, behavioral effects of PPN optogenetic stimulation and control optogenetic procedures. A and B. Top row: additional immunofluorescence histology sections illustrating ChR2 expression (magenta) and optic fiber placement in PPN (white dashed line) for animals where stimulation elicited running (**A**) or freezing (**B**). The anatomical boundary of PPN (white dashed line) was defined with ChAT immunofluorescence (cyan). White arrows: tip of the optic fibre. Scale bars: 500 µm. Top right in **B**: Individual (gray line) and group-average (orange line) decrease of running speed between epochs of baseline (-5 to 0 s, before laser onset) and stimulation (0 to 5 s, after laser onset), for the minority of 4 ChR2-expressing animals that displayed slowed locomotion or freezing behavior during PPN optogenetic stimulation (averaged over 7-10 stimulation sessions). Middle and bottom rows: change of average running speed during PPN optogenetic stimulation (laser ON, blue window) for the animals shown in top row, in a representative single recording session (middle row; gray line, mean ± SEM), or averaged over 10 sessions (bottom row; gray line, single recording session; orange line, mean ± SEM of all single sessions). Note the consistency of behavioral responses across multiple sessions for all animals. ** $P < 0.01$, *** $P < 0.001$, Wilcoxon signed rank test between pre-stimulation and stimulation epochs. **C**. Approximate optic fiber positions for all rats tested with PPN optogenetic stimulation, color-coded by the effect of laser stimulation on locomotion (green = running; red = freezing). Dashed line indicates PPN (sagittal section). **D**. Sagittal fluorescence photomicrograph of a control rat injected in PPN (white dashed line) with AAV5-CamKIIa-EYFP that did not express ChR2 (magenta). Anatomical boundary of PPN was defined with ChAT immunofluorescence (cyan). Red square: high magnification ROI shown in inset. Note the presence of ChAT+/YFP+ neurons (white arrows). Scale bars: 500 µm. **E**. Overlay of individual patterns of virus expression observed in control rats (n = 4) after AAV5-CamKIIa-EYFP injections in PPN (black dashed line). At each ML level, the anatomical boundary of PPN was defined by the extent of ChAT immunofluorescence, after which the areas of virus expression for each animal were superimposed (in pink). Blue dots indicate the location of the optic fibres for each control rat tested with PPN stimulation. The location and extent of virus spread in control animals, showing better expression in the neuron soma, was used as a proxy to evaluate infection patterns in experimental animals injected in PPN with a ChR2-expressing virus. **F**. Changes in average running speed for a representative control animal with PPN optogenetic stimulation (laser ON, blue window; gray line, single sessions (n = 10); orange line, mean ± SEM of all single sessions; baseline speed = 16.2 ± 0.7 cm/s, stimulation speed = 16.4 ± 1.0 cm/s; $Z = 1.1$, $P = 0.29$, Wilcoxon signed rank test). G. Summary of number of unresponsive (white), excited (filled), and inhibited (dashed) cells recorded in both HDB (green) and MEC (blue), categorized according to the behavioral phenotype elicited by PPN stimulation (running, left; freezing, right). The numbers in the middle of the charts display the total numbers of recorded cells for each category.

Figure S6

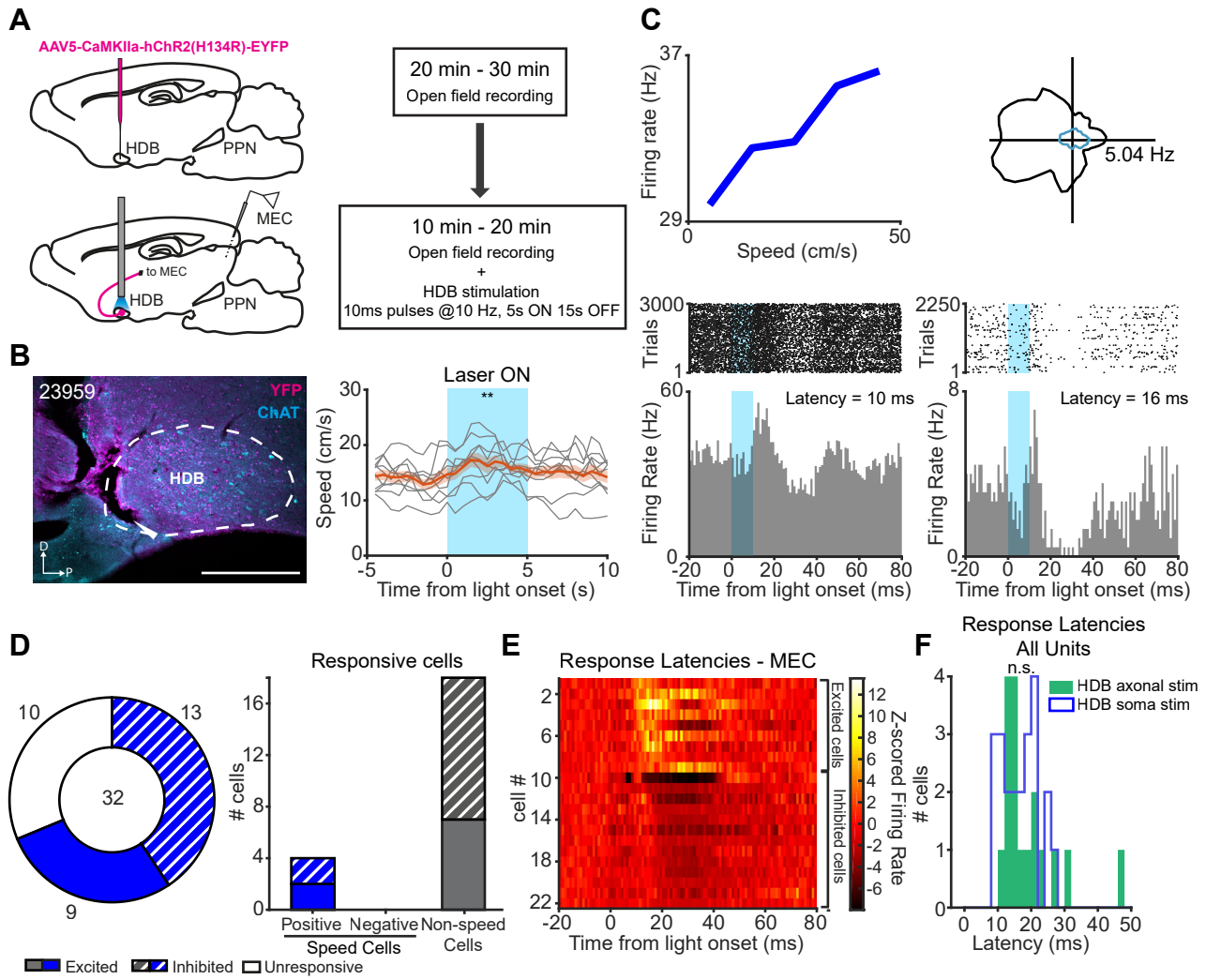
A
AAV5-CaMKIIa-hChR2(H134R)-EYFP
HDB
PPN
MEC
to MEC
HDB
PPN
20 min - 30 min
Open field recording
10 min - 20 min
Open field recording
+
HDB stimulation
10ms pulses @10 Hz, 5s ON 15s OFF
B
23959
YFP
ChAT
HDB
D
P
Laser ON
**
Speed (cm/s)
Time from light onset (s)
C
Firing rate (Hz)
Speed (cm/s)
5.04 Hz
Trials
Latency = 10 ms
Latency = 16 ms
Firing Rate (Hz)
Time from light onset (ms)
D
10
13
32
9
Responsive cells
cells
Positive
Negative
Speed Cells
Non-speed Cells
Excited
Inhibited
Unresponsive
E
Response Latencies - MEC
cell #
Excited cells
Inhibited cells
Z-scored Firing Rate
Time from light onset (ms)
F
Response Latencies
All Units
n.s.
HDB axonal stim
HDB soma stim
cells
Latency (ms)

Figure S6, related to Figure 6 | Direct optogenetic stimulation in HDB causes changes in MEC speed cell activity. A. Implantation and recording procedures. Left: AAV5-CamKIIa-hChR2(H134R)-EYFP was injected in HDB (n=1), followed by simultaneous implantation of an optic fiber in HDB, and tetrodes in MEC. Right: the recording protocol consisted of a baseline screening session in the open field, followed by a stimulation session with laser pulses delivered directly in HDB and activate a broad population of neurons and not exclusively those receiving PPN inputs. **B.** Left: sagittal fluorescence photomicrograph showing AAV5-CamKIIa-hChR2(H134R)-EYFP expression (magenta) and optic fiber placement in HDB. HDB anatomical border (white dashed line) is defined with ChAT immunofluorescence staining (cyan). White arrow indicates tip of the optic fibre. Scale bar: 500 µm. Right: average running speed during HDB optogenetic stimulation (laser ON, blue window) in a representative single recording session (gray line) and averaged over 10 sessions (orange line, mean ± SEM). ** $P < 0.01$, Wilcoxon signed rank test between pre-stimulation and stimulation epochs (baseline speed = 14.0 ± 0.9 cm/s, stimulation speed = 16.2 ± 1.0 cm/s; $Z = 2.8$, $P = 0.0051$, Wilcoxon signed rank test). **C.** Top: representative examples of speed and head tuning curves of a speed cell and head direction cell, respectively, recorded in MEC during the baseline session. Bottom: raster plots (top) and PSTH (bottom) for the cells shown in the top, displaying absolute changes in firing rate after the onset of optogenetic stimulation in HDB during the stimulation session. **D.** Left: total number of unresponsive (white), excited (blue) and inhibited (dashed blue) cells recorded in MEC, following direct HDB stimulation (centre: total number of recorded cells). Right: summary of positive speed cells (blue, excited; dashed blue, inhibited) and non-speed cells (gray, excited; dashed gray, inhibited) among responsive cells in MEC. **E.** Color-coded summary of changes in firing activity of all responsive cells recorded in MEC following direct HDB stimulation, sorted by response type (excitation/inhibition) and response latency. Z-scored firing rates are color-coded (scale bar). **F.** Histogram showing distribution of response latencies in all responsive cells in MEC following direct stimulation of HDB ('HDB soma stim', blue) compared to the response latencies of all MEC responsive units tested during stimulation of PPN axonal terminals in HDB ('HDB axonal stim', green).

Supplemental Table S1, related to Figure 4 | Number of cells in HDB responsive to PPN stimulation. Summary table discriminating, for each animal used in optogenetic experiments, the total number of recorded cells in HDB, total number of cells responsive to PPN stimulation, and numbers of PPN-responsive cells according type of speed modulation (positive speed cell, negative speed cell, non-speed cell).

Animal	Recorded Cells	Non-modulated Cells	Modulated Cells	Positive Speed Cells	Negative Speed Cells	Non-speed Cells
22698	19	11	8	0	1	7
22699	15	3	12	6	2	4
22700	38	15	23	3	4	16
22701	19	2	17	3	3	11
23084	25	10	15	2	6	7
23085	26	2	24	10	3	11
23590	1	1	0	0	0	0
23591	19	6	13	1	3	9

Supplemental Table S2, related to Figure 4 | Number of cells in MEC responsive to PPN stimulation. Summary table discriminating, for each animal used in optogenetic experiments, the total number of recorded cells in MEC, total number of cells responsive to PPN stimulation, and numbers of PPN-responsive cells according to type of speed modulation (positive speed cell, negative speed cell, non-speed cell) and cell identity (putative principal cell, pPC; putative interneuron, pINT).

				Positive Speed Cells		**Negative Speed Cells**		**Non-Speed Cells**	
Animal	**Recorded Cells**	**Non-modulated Cells**	**Modulated Cells**	**pPC**	**pINT**	**pPC**	**pINT**	**pPC**	**pINT**
22589	18	14	4	0	3	0	0	1	0
22698	12	12	0	0	0	0	0	0	0
22699	38	30	8	0	4	0	0	2	2
22700	41	34	7	0	4	0	0	2	1
22701	10	9	1	0	0	0	0	0	1
23084	9	9	0	0	0	0	0	0	0
23590	27	21	6	0	1	0	1	1	3
23591	21	13	8	0	3	0	1	1	3
23678	18	17	1	0	1	0	0	0	0
23679	5	4	1	0	0	0	0	0	1
23943	16	10	6	0	3	0	1	2	0
24005	10	10	0	0	0	0	0	0	0
24179	69	54	15	0	6	0	0	2	7
24181	49	41	8	1	6	0	0	1	0
24192	23	17	6	0	3	0	0	3	0
23957	This animal was only used to assess the behavioral effects of PPN stimulation as tetrodes were not located in MEC								